energies

MDPI

Article

Design, Simulation and Experimental Investigation of a Solar System Based on PV Panels and PVT Collectors

Annamaria Buonomano, Francesco Calise * and Maria Vicidomini

Department of Industrial Engineering (DII)—University of Naples Federico II, P.le Tecchio, 80, Naples 80125, Italy; annamaria.buonomano@unina.it (A.B.); maria.vicidomini@unina.it (M.V.)
* Correspondence: frcalise@unina.it; Tel.: +39-081-7682301

Academic Editor: Maurizio Sasso
Received: 11 April 2016; Accepted: 21 June 2016; Published: 29 June 2016

Abstract: This paper presents numerical and experimental analyses aimed at evaluating the technical and economic feasibility of photovoltaic/thermal (PVT) collectors. An experimental setup was purposely designed and constructed in order to compare the electrical performance of a PVT solar field with the one achieved by an identical solar field consisting of conventional photovoltaic (PV) panels. The experimental analysis also aims at evaluating the potential advantages of PVT vs. PV in terms of enhancement of electrical efficiency and thermal energy production. The installed experimental set-up includes four flat polycrystalline silicon PV panels and four flat unglazed polycrystalline silicon PVT collectors. The total electrical power and area of the solar field are 2 kWe and 13 m^2, respectively. The experimental set-up is currently installed at the company AV Project Ltd., located in Avellino (Italy). This study also analyzes the system from a numerical point of view, including a thermo-economic dynamic simulation model for the design and the assessment of energy performance and economic profitability of the solar systems consisting of glazed PVT and PV collectors. The experimental setup was modelled and partly simulated in TRNSYS environment. The simulation model was useful to analyze efficiencies and temperatures reached by such solar technologies, by taking into account the reference technology of PVTs (consisting of glazed collectors) as well as to compare the numerical data obtained by dynamic simulations with the gathered experimental results for the PV technology. The numerical analysis shows that the PVT global efficiency is about 26%. Conversely, from the experimental point of view, the average thermal efficiency of PVT collectors is around 13% and the electrical efficiencies of both technologies are almost coincident and equal to 15%.

Keywords: experimental; dynamic simulation; PVT collectors; PV panes

1. Introduction

In the last years particular attention has been paid to the development of economically viable solar thermal and electrical systems, with the twofold aim at improving power density and reducing system capital costs. As well known, for a long time the massive development of solar technologies has been limited by their poor economic profitability due to the high system capital costs.

Nevertheless, the recent remarkable decrease of capital costs of solar thermal collectors (SC) and photovoltaic (PV) panels and the simultaneous increase of sustainable energy policies, adopted by the majority of governments worldwide, are promoting more and more the uptake of small-scale solar systems. Among European Union countries, one of the goals of the established energy policies is to achieve a widespread adoption of small SC and PV systems, in order to enhance the utilization of renewable energy sources [1,2].

In this framework, photovoltaic/thermal (PVT) collectors are particularly promising due to their combination of conventional PV and SC collectors in a single component [3,4]. PVT collectors are

typically manufactured by using a conventional thermal collector whose absorber is covered with a suitable PV layer. The thermal energy is distributed to a fluid, typically air [5] or water [6–8], whereas the PV layer produces electricity [3,4]. The overall result of this technology is a simultaneous production of electricity and heat [9], with a reduction of the PV modules' electrical efficiency losses.

In fact, the electrical efficiency of a PVT collector may be even higher than that of a conventional PV panel given moderate PVT operating temperature increases [3,4,10]. In order to study the effect of the operating temperature on the electrical and thermal efficiencies, numerous numerical and experimental works on this topic were carried out in the last years [11–13]. Kalogirou and Tripanagnostopoulos [14] carried out a numerical simulation analysis of the energy performance of two PVT collector models (one made from polycrystalline silicon, pc-Si, and another with amorphous silicon, a-Si) for three locations at different latitudes (Nicosia, Athens and Madison). The obtained results (also tested experimentally) showed that although a PV system produces about 38% more electrical energy, the studied PVT system also covers, depending on the location, a large percentage of the hot water needs. Aste et al. [6] designed an experimental innovative water glazed PVT component, consisting of a thin film PV technology and a roll-bond flat plate absorber, and developed a mathematical model for the prediction of the electrical and thermal outputs. Through such a model, validated by means of the obtained experimental data, the daily mean electrical efficiency of the PVT resulted to be about 6.0%, whereas the PV module showed a daily average efficiency of 6.2%. The PVT collector also produced thermal energy, with a daily efficiency of 25.8%. Touafek et al. [15] modelled and simulated a novel design of a PVT collector including an absorber plate integrated with sheet galvanized steel. The advantages of this collector with respect to other configurations are better heat absorption and lower production cost. The simulation model allows assessing the temperatures levels of such layers and the effect of some parameters on the electrical and thermal performances. The authors also compared the prototype collector's performance with that of existing configurations. Fan et al. [16] reported the results of a 10 months experimental analysis of a 900 Wp liquid type glazed mc-Si PVT system, developed in Singapore. The analysis carried out on the operational data showed that the PVT system is capable of achieving 41.1% of the average monthly conversion efficiency. Dry and wet stagnation tests were also performed, showing that the maximum temperature of the water under dry and wet stagnation conditions was 64 °C and 65 °C, respectively. Herrando and Markides [17] developed a numerical model of a water cooled PVT collector in order to estimate the year-long techno-economic performance of the system for a typical house in London, UK. The results showed that for the simulated low solar irradiance levels and low ambient temperatures, a higher coverage of total household energy demands and higher CO_2 emission savings can be achieved through the complete coverage of the solar collector with PV and a relatively low collector cooling flow-rate. They concluded that hybrid PVT systems offer a notably improved proposition over PV-only systems [18]. Guo et al. [19] reported the results obtained through a simulation model of a novel tri-functional PVT collector, validated by means of experimental data. The investigated collector operates in PV/water-heating and PV/air-heating modes, as a function of the energy demands. The authors highlighted the good consistency between simulation and experimental results, showing also that the tri-functional PVT collector is more efficient than a disjointed configuration of a PVT water and air collector. In addition, the authors also investigated the collector performance under different flow rates, wind speeds, inlet air temperatures, initial water temperatures, as well as the annual thermal efficiencies of such collector in three different climates in China (38.5%, 38.9%, and 40.1% in Hefei, Beijing, and Xining, respectively). Sardarabadi et al. [20] experimentally investigated the effects of adding nanofluids (SiO_2/pure water, 1 wt % and 3 wt %) as a coolant flowing through the flat plate PVT collector from both energetic and exergetic points of view. Daily experiments were performed for the PVT system, tilted by 32° and under constant mass flow rates. The results showed that silica/water nanofluid suspension significantly enhanced the energetic and exergetic performances of the system, showing an increase of overall energy efficiency by up to 7.9% and of total exergy by up to 24.31%.

As mentioned before, a number of papers available in the literature have investigated several PVT collectors from both numerical and experimental points of view. However, only a few papers couple experimental analyses with 1-year simulation models of the system. In addition, none of the investigated papers present an integrated approach aiming at comparing PVT vs. PV technologies, from both numerical and experimental points of view.

In this framework, this paper aims to cover this lack of knowledge, reporting numerical and experimental studies where a PVT solar field is compared, from both energetic and economic points of views, with a PV field (identical PV modules and different PVT collectors are simulated/experimented). Note that simulations and experiments were carried out by taking into account the same PV types, whereas different PVT technologies were considered. Specifically, the experimented PVTs collectors are unglazed types, consisting of the same PV models in combination with water heat extraction units. Differently, in order to evaluate the performance of the novel generation of PVTs, represented by glazed devices, an additional comparison with the PVs was carried out by means of dynamic simulations. In fact, this paper presents the design of an experimental set-up, consisting of PVT collectors and PV panels, as well as the results obtained through the thermo-economic dynamic simulation model, developed for the analysis and comparison of energy performance, are discussed. In particular, the experimental set-up, installed at the company AV Project Ltd., located in Avellino (Italy), consists of four flat polycrystalline silicon PV panels and four flat polycrystalline silicon PVT collectors (named Janus). The designed experimental set-up allows gathering the systems electrical and thermal efficiencies as well as the temperatures reached by both solar technologies (PV and PVT), in order to determine: (i) the technology showing the higher performance; (ii) validate the dynamic simulation model by comparing the obtained results with experimental ones.

2. Numerical Model

2.1. System Layout

The modelled system was developed in order to dynamically simulate the energy performance of an experimental set-up consisting of four glazed flat-plate solar PVT collectors and four polycrystalline silicon PV panels for the production of domestic hot water and electricity. The set-up also includes a water stratified vertical storage tank, with an internal heat exchanger. The simulation system layout, based on the experimental set-up, is depicted in Figure 1 and includes three main system loops:

- SCF: Solar Collector Fluid loop, related to the water flowing between the solar field and the storage tank through the HE1, supplied by a water constant speed pump, P1;
- DHW: Domestic Hot Water loop, related to the outlet water from storage tank TK and supplied directly to the users or mixed through a tee piece (TP), with tap water to the DHW set point temperature;
- TW: Tap Water loop, related to the grid water supplied by temperature controlled liquid flow diverter (FD) to storage tank or to tee piece.

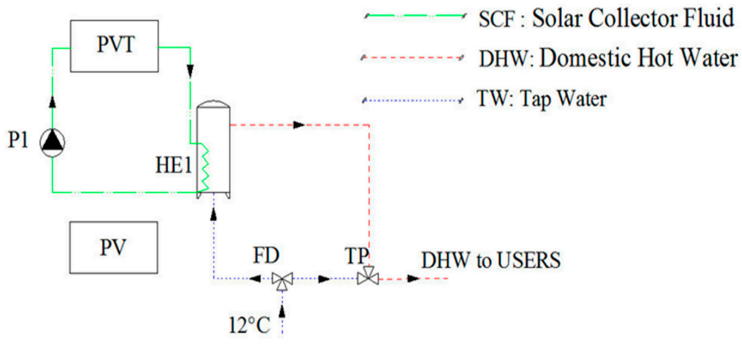

Figure 1. Plant layout. Use same font size in legends labels.

The operating principle of the system under investigation and the related control strategies can be summarized as follows: PVT collectors are managed by a controller operating on the P1. This controller receives temperature readings from the outlet of HE1 (i.e., solar collector inlet temperature) and the outlet pipe of the solar collector loop. Hot water (produced by the solar loop) supplies heat to the TK by HE1. The controller stops the pump P1 if the solar collector outlet temperature is lower than the inlet one, in order to avoid any heat dissipation and if the incident total radiation is lower than 10 W/m^2. Another controller manages the activation of the temperature controlled liquid flow diverter for the tap water inlet in the system. In particular, the controller receives temperature measurements from the top of TK and the set point temperature for DHW (TTK_{topSET}) and produces the ON signal (i.e., activation of temperature controlled liquid flow diverter) if the TK top temperature is higher than TTK_{topSET} + 3 °C or lower than TTK_{topSET} − 3 °C. Obviously, tap water flows enters the system if DHW is required. By means of the temperature controlled liquid flow diverter, tap water is supplied directly to the TK if the TK top temperature is lower than TTK_{topSET}, whilst it is mixed with outlet hot water from the TK by the tee piece, TP. This prevents too high DHW temperatures. Then, outlet mixed water from TP or outlet hot water from TK can be used by the home occupants for DHW purposes.

2.2. Simulation Model

In order to compare the obtained numerical data (e.g., electrical, thermal efficiency, temperatures reached by both solar technologies) with measurements, the developed simulation model was dynamically simulated by means of the software TRNSYS. It includes a library of built-in components (e.g., pumps, mixers, diverters, valves, controllers, auxiliary heater, heat exchanger, etc.) often based on experimental data [21]. For a detailed description of the main utilized components models, see the TRNSYS references related to Type 3b for the constant speed pump P1, Type 11 for the temperature controlled liquid flow diverter and the tee piece [21]. The TRNSYS built-in Type 340 stratified fluid storage tank, with four optional internal heat exchangers and ten connections (double ports), for direct charge and discharge of the tank, is adopted. In particular, in this model, one double port and one heat exchanger are adopted: the double port of TK is supplied by tap water for producing DHW; heat exchanger HE1 charges the TK with the heat produced by PVT collectors. This methodology has been successfully adopted to perform dynamic analyses of several solar systems [22,23]. In this section, only a brief description of the most significant models, Type 94 for the PV panels, Type 50 for the PVT collectors, is provided. The design and operating parameter assumptions for the PVT collectors, PV panels and storage tank are listed in Table 1.

Table 1. Main parameters used in the model.

Parameter	Description	Value	Unit
PVT Solar Collector			
A_{PVT}	PVT Solar Collector area	6.5	m^2
q_{P1}/A_{PVT}	P1 rated flow rate per unit of PVT area	50	kg/m^{2}h
F′	Collector Fin Efficiency Factor	0.6	-
α	Collector plate absorptance	0.8	-
U_L	Collector thermal loss coefficient	25	W/m^{2}K
τ	Cover transmittance	0.99	-
C	Temperature coefficient of solar cell efficiency	0.0032	-
T_{ref}	Reference temperature for cell efficiency	25	°C
PF	Packing factor	0.8	-
PV Solar Panels			
A_{PV}	PV Solar Panel area	6.5	m^2
$I_{sc,ref}$	Module short-circuit current at reference conditions	8.493	A
$V_{oc,ref}$	Module open-circuit voltage at reference conditions	37.62	V
$T_{c,ref}$	Reference temperature	298	K

Table 1. *Cont.*

Parameter	Description	Value	Unit
$G_{T,ref}$	Reference insolation	1000	W/m^2
$V_{mp,ref}$	Module voltage at max power point and reference conditions	31.78	V
$I_{mp,ref}$	Module current at max power point and reference conditions	7.898	A
μ_{Isc}	Temperature coefficient of I_{sc} at (ref. condition)	0.00049	-
μ_{voc}	Temperature coefficient of V_{oc} (ref. condition)	−0.0033	-
$T_{c,NOCT}$	Module temperature at NOCT	319	K
$T_{c,ref}$	Ambient temperature at NOCT	293	K
Ns	Number of individual cells in module	6	-
NS	Number of modules in series	4	-
Tank			
H_{TK}	Height	1.76	m
V_{TK}/A_{PVT}	Tank Volume per unit of PVT area	50	L/m^2
q_{HE1}/A_{PVT}	Heat Exchanger 1 flow rate per unit of PVT area	50	kg/m^2h
TTK_{topSET}	Tank top set temperature	55	°C
q_{DHW}	Domestic Hot Water flow rate	325	L/day

2.2.1. PV Panels

In order to simulate the polycrystalline PV panels, the so-called "four parameter" model of Type 94 is used [24–26]. It assumes that the slope of the IV curve is zero at the short-circuit condition, see Equation (1):

$$\left(\frac{dI}{dV}\right)_{v=0} = 0 \tag{1}$$

The four parameters included in the model are: (i) $I_{L,ref}$ (module photocurrent at reference conditions); (ii) $I_{0,ref}$ (diode reverse saturation current at reference conditions); (iii) γ (empirical PV curve-fitting parameter); (iv) R_s (module series resistance). Type 94 calculates these values from manufacturers' data in order to generate an IV curve at each time step.

The current-voltage equation of circuit is shown in Equation (2):

$$I = I_{L,ref}\frac{G_T}{G_{T,ref}} - I_0\left[\exp\left(\frac{q}{\gamma k T_c}(V + IR_s)\right) - 1\right] \tag{2}$$

The reference insolation $G_{T,ref}$ is nearly always defined as 1000 W/m^2. The diode reverse saturation current I_0 is a temperature dependent quantity, calculated as in Equation (3):

$$\frac{I_0}{I_{0,ref}} = \left(\frac{T_c}{T_{c,ref}}\right)^3 \tag{3}$$

Once I_0 is obtained, the Newton's method is employed to calculate the PV current. In addition, an iterative search routine finds the current (I_{mp}) and voltage (V_{mp}) at the point of maximum power along the IV curve. Calculation algorithms used to solve the four equivalent circuit characteristics are discussed in the following. By substituting the current and voltage into Equation (2) at the open-circuit, short circuit, and maximum power conditions and then by considering some rearrangement yields the following three Equations (4) and (5) related to $I_{L,ref}$, $I_{0,ref}$, γ:

$$I_{L,ref} \approx I_{sc,ref} \tag{4}$$

$$\gamma = \frac{q\left(V_{mp,ref} - V_{oc,ref} + I_{mp,ref}R_s\right)}{kT_{c,ref}\ln\left(1 - \frac{I_{mp,ref}}{I_{sc,ref}}\right)} \tag{5}$$

$$I_{0,ref} = \frac{I_{sc,ref}}{\exp\left(\frac{qV_{oc,ref}}{\gamma k T_{c,ref}}\right)} \quad (6)$$

At this point, a fourth equation, Equation (7), derived by taking the analytical derivative of voltage with respect to temperature at the reference open-circuit condition, is needed in order to determine the last unknown parameter:

$$\frac{\partial V_{oc}}{\partial T_c} = \mu_{voc} = \frac{\gamma k}{q}\left[\ln\left(\frac{I_{sc,ref}}{I_{0,ref}}\right) + \frac{T_c \mu_{isc}}{I_{sc,ref}} - \left(3 + \frac{q\varepsilon}{\frac{\gamma}{N_s} k T_{c,ref}}\right)\right] \quad (7)$$

This analytical value is matched to the open circuit temperature coefficient (manufactures' specification). Finally, an iterative search routine is followed to calculate the equivalent circuit characteristics [21].

2.2.2. PVT Collectors

In order to model the glazed PVT collectors, the Type 50 is used [21]. In TRNSYS, the PVT model was obtained by coupling a PV module to the standard flat-plate solar collector, modeled by Type 1. It simulates a combined collector and incorporates both the analysis and work of Florschuetz [27] for flat plate collectors operated at peak power, and the analysis of Evans et al. [28], for concentrating combined collectors. The latter analysis makes use of the I–V curves of the cells (or array) in solving for peak power or for current output at some imposed voltage. In this analysis for calculating the thermal losses of collectors, constant loss coefficient (U_L) and transmission coefficient (τ) are used. Note that the model implemented in Type 50 is based on an extension of the Hottel-Whillier model for the analysis of combined photovoltaic/thermal flat plate collectors (actually there is no official standard testing for PVT collectors [29]). The characteristics of such method are the collector fin efficiency factor, F', and the overall transmittance-absorptance product, $\tau\alpha$, whose parameters are reported in Table 1.

2.3. Economic Model

A detailed economic model was also developed in order to assess the economic profitability of the systems (PVT system and PV system) under investigation. The economic savings achieved by the proposed systems were assessed by comparing the systems' capital and operating costs to those of a so-called reference system, (RS). In the considered reference system it was assumed that DHW and electricity are provided by the gas boiler (GB) and the national grid, respectively. The proposed systems yearly savings, ΔC_{PV} and ΔC_{PVT}, are reported in terms of operating costs, compared to those of the reference configuration, RS, and the maintenance cost, estimated as 2% of total capital cost. The yearly savings are calculated in Equations (8) and (9):

$$\Delta C_{PV} = E_{PV,el} \times c_{el} - M_{PV} \quad (8)$$

$$\Delta C_{PVT} = E_{PVT,el} \times c_{el} + \frac{E_{DHW,th} \times c_{NG}}{\eta_{GB} \cdot LCV} - M_{PVT} \quad (9)$$

where: $E_{PVT,el}$ and $E_{PV,el}$ (kWh/year) are the useful electricity produced by the PVT and PV, respectively; $E_{DHW,th}$ (kWh/year) is the energy consumption of the gas boiler for producing DHW; η_{GB} is the thermal efficiency of the gas boiler; c_{el} is the electricity cost (€/kWh); LCV is lower calorific value of natural gas (kWh/Sm^3); c_{NG} is the thermal energy cost, assessed in terms of natural gas one (€/Sm^3); M is maintenance cost (€/year).

The total capital costs (considering installation costs) of the proposed systems include, respectively, the PVT solar field, pump, tank and connection pipes for PVT system ($C_{tot,PVT}$) and PV panels for PV system ($C_{tot,PV}$). The specific cost per m^2 of PVT collectors and PV panels was estimated in 769 and 366 €/m^2, respectively, from the manufacturer catalog data of the AV Project Ltd. company (Avellino, Italy) [24].

The costs of plant sensors (flowmeters, pyranometer, thermoresistances, thermocouples, power optimizer and monitoring system) is not included. All component costs are listed in Table 2. The economic profitability analysis for both systems also includes the assessment of the Simple Pay Back period, (SPB_{PVT}, SPB_{PV} in Equation (10)), the Net Present Value (NPV_{PVT}, NPV_{PV} in Equation (11)), and the Profit Index (PI_{PVT}, PI_{PV} in Equation (12)) also by considering possible public funding in terms of capital cost contribution.

Table 2. Costs of the components.

Component	Cost (€)
PVT collectors	5000
Pump and controller	125
Tank	350
Connection pipes	100
PV panels	2380

Such assumption is compliant with the Italian legislation [25], which expects for the installation of solar collectors or PV panel a public funding equal to 50% of total capital cost:

$$SPB_{PVT} = \frac{C_{tot,PVT}}{\Delta C} \; SPB_{PV} = \frac{C_{tot,PV}}{\Delta C} \tag{10}$$

$$NPV_{PVT} = AF \cdot \Delta C_{PVT} - C_{tot,PVT} \; NPV_{PV} = AF \cdot \Delta C_{PV} - C_{tot,PV} \tag{11}$$

$$PI_{PVT} = \frac{NPV_{PVT}}{C_{tot,PVT}} \; PI_{PV} = \frac{NPV_{PV}}{C_{tot,PV}} \tag{12}$$

3. Experimental Set-Up

The main components of the experimental set-up, shown in Figure 2, are:

- flat polycrystalline silicon PV panels, for the production of electricity;
- flat polycrystalline silicon unglazed PVT solar collectors (called Janus), for the production of electricity and thermal energy (Figure 3). Basically, a Janus collector is made by an aluminium plate integrated with a conventional PV panel by a thin butyl layer. A particular solution of water + glycol was selected in order to avoid corrosion and freezing risk. The design features of Janus collectors are reported in Table 3.

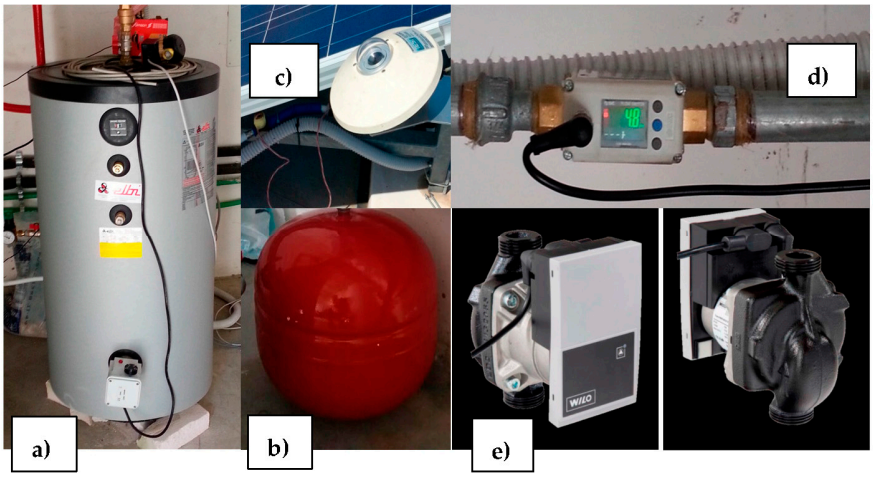

Figure 2. (**a**) BSV-200 Elbi storage tank; (**b**) expansion vessel; (**c**) LP PYRA 02 AC pyranometer; (**d**) SMC LFE 1D4F1 flowmeter; (**e**) WILO Yonos PARA ST 7.0 PWM2 flow rate pump.

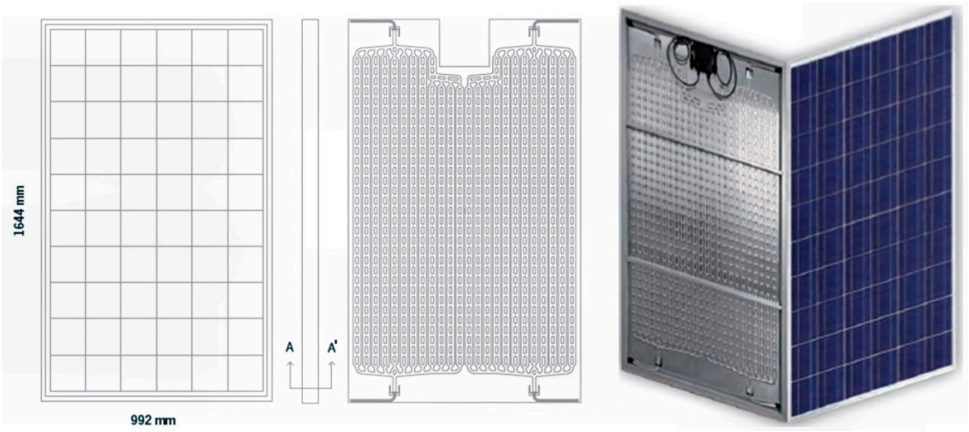

Figure 3. *Janus* PVT collector.

Table 3. Design features of PVT Janus collector, water circulation pump.

Features	Values/Units
Janus PVT Collector	
Thermal production	≈400 Wh/m^2
Operation maximum pressure	600 kPa
Operation maximum temperature	90 °C
Fluid volume	0.9 L
Maximum flowrate	100 L/h
Diameter of connection pipes	Inner: Φ 8 × 1 mm/Outer: Φ 12 × 1 mm
Connection pipes	4 cross-linked polyethylene pipes (2 loops)
Collector elements number	48 channels of 10 mm
Absorber surface	1.44 m^2
Solar collector total surface	1.63 m^2
Solar collector Weight	25.02 kg
WILO Yonos PARA ST 7.0 PWM2 Pump	
Maximum flowrate	3.2 m^3/h
Operation maximum pressure	1 MPa
Head	7.0 m
Nominal diameter	15 mm

The total electrical power of the solar field, consisting of four PV panels and four PVT solar collectors, is 2 kWp (250 Wp per module). Other components are:

- heat storage tank, (BSV ELBI vitrified tank, capacity: 200 L; maximum operating pressure: 1 MPa; operating maximum temperature: 95 °C, Figure 2). It includes: (i) an internal fixed one-pipe heat exchanger (surface area: 0.7 m^2; capacity: 5 L; maximum operating pressure: 1.2 MPa; maximum operating temperature: 110 °C) used to exchange heat with the water tank, by means of the outlet hot water supplied by the Janus collectors; (ii) an internal optional electrical resistance (with thermostat, 2 kW) for eventually heat up the water tank to the set point temperature;
- connecting pipes, (multilayer pipes, inner diameter 15 mm; outer diameter: 20 mm), for connecting the collectors to the coil of the storage tank;
- water pump, (WILO Yonos model) for the circulation of the fluid from the internal heat exchanger of heat storage tank to inlet solar collectors. In order to meet the total loss of pressure, carefully calculated (about 3.30 m of distributed and concentrated losses of pressure, due to the fluid circulation through the collectors and the internal heat exchanger of the storage tank) the WILO Yonos PARA ST 7.0 PWM2 pump was selected. Design features of WILO Yonos pump are reported in Table 3.

- expansion vessel, (nominal volume: 33 L; maximum pressure: 300 kPa) allowing the expansion of fluid by avoiding the overpressures due to fluid volume growth caused by the increasing fluid temperatures;
- flowmeter, (SMC LFE 1D4F1 model, range of flowrate reading: 0.5–20 L/min; range of operation temperature: 0–85 °C) for measuring the fluid flow rate;
- pyranometer, (LP PYRA 02 AC model, maximum radiation value: 2000 W/m^2, temperature operation range from −40 °C to 80 °C) for measuring the solar radiation;
- thermoresistances and thermocouples, for measuring the temperature.

In order to store and process the gathered data by measurements instruments, a Multicon Simex CMC14 data logger, capable to simultaneously measure and control several system parameters, was selected (Figure 4a).

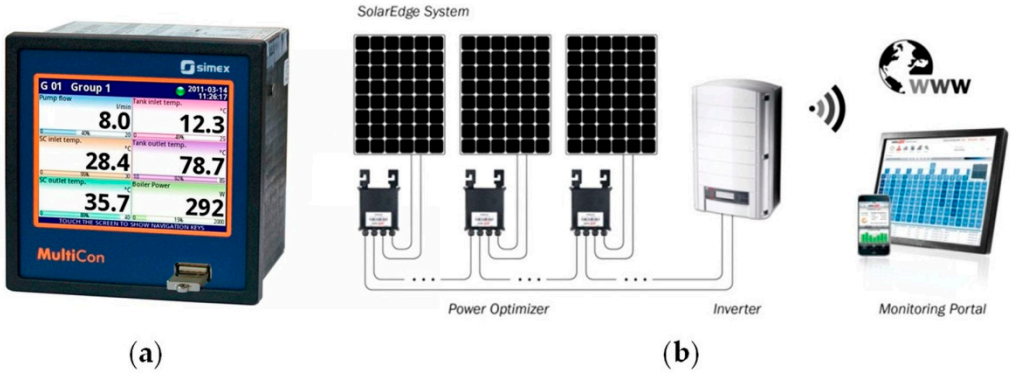

Figure 4. (**a**) Multicon Simex CMC141 data logger; (**b**) SolarEdge System.

Finally, such experimental set-up also includes a SolarEdge system (Figure 4b) that provides highly efficient single-phase inverters, power optimizers, for maximizing the energy production from each PV module, and a system for monitoring in real time the panel performance. The whole system layout is shown in Figure 5. A further important experiment for obtaining the PVT collectors' and PV panels' operating temperatures was carried out by means of an infrared camera (FLIR T335. Range: −20 to +650 °C, accuracy: ±2%, IR resolution: 320 × 240 pixels). The camera allows measuring the temperature of each point of the image, consisting of a matrix of pixels. The colour of each pixel suitably represents a temperature measurement. The technical features of the set of meters are summarized in Table 4.

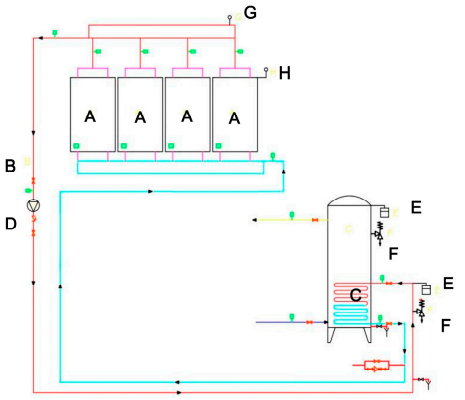

	Solar collectors outlet fluid
	Solar collectors inlet fluid
	Domestic Hot Water
	Tap water
	Pex pipes
A	PVT collectors Janus
B	Pipes
C	Storage tank
D	Pump
E	Expansion vessel;
F	Security valve
G	Venting valve
H	Pyranometer

Figure 5. Experimental set-up layout.

Table 4. Technical features of the set of meters.

Parameters	Values/Units
Data Logger Multicon Simex	
Supply voltage	Module PS42: voltage 85–260 V ca.
Consume	25 VA; max 35 VA
Display	TFT 5.7″ resolution touchscreen, 320 × 240 pixel, 16 bit
Sensor power supply output	24 V cc ± 5%/max 200 mA
Communication interface	RS-485 Modbus RTU; USB
Digital input	24 Vcc
Communication Module	Slot D: Module "ETU" of communication, USB port and Ethernet
Input Modules	Slot B: Module "R81" 8 relè to 1 A Slot C: Module "I24" 24 analogic inlets in current 0/4–20 mA
Output Module	Slot A: Module "IO6" 6 analogic outlets in current 4–20 mA
Internal Memory	1.5 Gb
Operation Temperature	0 to 50 °C
Storage Temperature	−10 to 70 °C
Humidity	5% to 90%
Altitude	2000 m
Size	(144 × 144 × 100) mm
LP PYRA 02 AC Pyranometer	
Maximum radiation value	2000 W/m^2
Temperature operation range	−40 to 80 °C
Off-set of zero	25 W/m^2
Impedance	5–55 Ω
SMC LFE 1D4F1 Flowmeter	
Range of flowrate reading	0.5–20 L/min
Range of operation temperature	0 to 85 °C
Detection Method	Electrostatic capacity
Range of operating pressure	0–1 MPa
Digital output	Maximum current: 80 mA, Maximum voltage: 28 VDC
Temperature Sensors	
PT100: Range of operation temperature	−50 to 200 °C
Thermocouples K: Range of operation temperature	−50 to 150 °C

4. Numerical and Experimental Results

As mentioned before, the final aim of this paper is to compare the newer PVT technology, consisting of glazed collectors, with the more traditional PV panels. In particular, two types of analyses were carried out: a numerical one, based on a 1-year dynamic simulation of the two systems under investigation, and an experimental one, aimed at comparing the real performance of PVs and PVTs collectors, consisting of the same PV models in combination with water heat extraction units. In both cases, the obtained results are analysed from energetic and economical points of views. It is worth noting that the two approaches are strictly related since the input parameters of the numerical models are those of to the experimental set-up under investigation. The following sections first report the results of the numerical analyses and subsequently the experimental test ones.

4.1. Numerical Results

4.1.1. Yearly Analysis

A discussion about the obtained experimental and simulation results is reported in this section. The electrical energy produced by the PV panels, Eel PV, equal to 1778 kWh/year, is greater than that, Eel PVT, produced by the PVT collectors, which also provide thermal energy used for DHW purposes. The electrical efficiency of PV panels reaches about 18%, whereas that of PVT collectors is about 12% (Table 5). This remarkable difference is due to the fact that the average PVT operating temperature is higher than the PV one, causing such a remarkable decrease of the electrical efficiency. In fact, PVT collectors are forced to operate to higher temperatures compared to PV ones (especially in winter and

in middle seasons) in order to supply the required DHW. On the other hand, the global efficiency of PVT collectors, as the sum of their electrical and thermal efficiencies, is equal to about 26%. In other words, the reduction in thermal efficiency is counterbalanced by the PVT thermal production. The total capital cost of the proposed PVT system (including PVT collectors, tank, pump and connection pipes) is 5575 €; the total capital cost of the proposed PV system (including PV panels) is 2380 €. The economic savings due to the electricity production by PV panels is about 296 €/year, whereas the economic saving due to the electricity and thermal energy production by PVT collectors is about 650 €/year (Table 6). Without the capital cost contribution (assumed in this analysis equal to 50% of total capital cost), the SPB, 8 and 7 years for PVT and PV system, respectively, are similar. Obviously, when the capital cost contribution is taken into account, the SPB decreases to about 4 years. Therefore, the economic profitability of both systems is better. In Table 6 the economic results regarding the case of capital cost contribution are shown.

Table 5. Yearly energy results.

kWh/Year			%		
E_{el} *PVT*	E_{th} *PVT*	E_{el} *PV*	η_{el} *PVT*	η_{th} *PVT*	η_{el} *PV*
1156	1433	1778	11.6	14.4	17.9

Table 6. Yearly economic results.

€		€/Year		€		Years			
$C_{tot\ PVT}$	$C_{tot\ PV}$	ΔC_{PVT}	ΔC_{PV}	NPV_{PVT}	NPV_{PV}	SPB_{PVT}	SPB_{PV}	PI_{PVT}	PI_{PV}
2788	1190	650	296	5340	2513	4	4	1.9	2.1

4.1.2. Weekly Analysis

The electrical power produced by PV panels, Eel PV, the thermal and electrical power produced PVT collectors, Eth PVT and Eel PVT, the global incident solar radiation, *G*, are shown on a weekly basis in Figure 6. By following the incident solar radiation, similar trends for the electricity and thermal production can be obtained. During summer, Eel PV is much higher than Eel PVT, whereas during winter this difference decreases. In addition, the production of thermal energy (Eth PVT) is comparable to the electrical ones produced by PVT and PV.

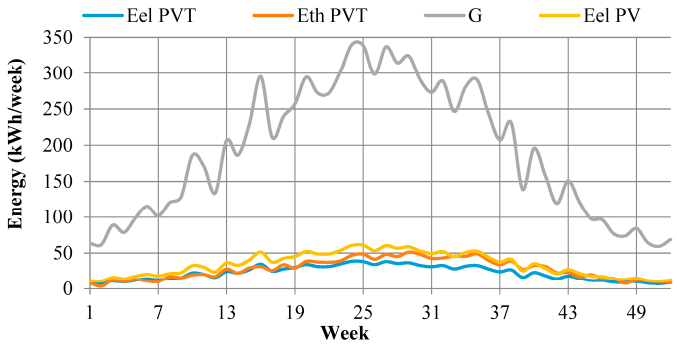

Figure 6. Weekly energy trends.

4.1.3. Daily Analysis

For the investigated system, Figure 7 shows, for a typical summer day (28 July), the thermal, Pth PVT, and power production, Pel PV and Pel PVT, on the left vertical axis, and the related efficiencies, ηel PV (i.e., PV panels), ηth PVT and ηel PVT (PVT collectors), on the right one. In the same figure,

the global solar radiation, *G*, is also depicted for suitable evaluation of the electrical and thermal efficiencies with respect to solar radiation.

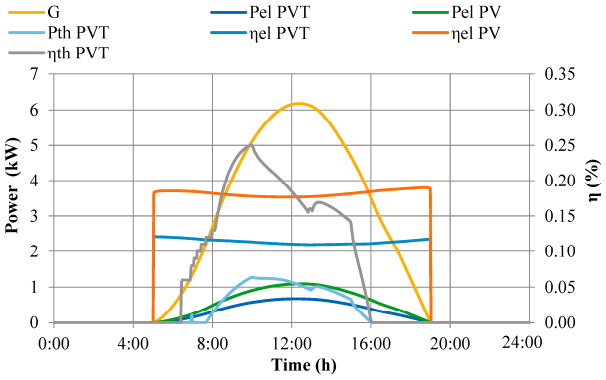

Figure 7. Daily power (left) and efficiency (right).

When global solar radiation hits the solar panels and collectors, between 5:00 a.m. and 6:00 p.m., the trend of PV and PVT electrical efficiencies is almost constant, equal to 19% and 12%, respectively. Such efficiencies slightly decrease (e.g., during the central hours of the day) due to the increase of the solar cells temperatures caused by the peak of solar radiation and outdoor temperature. On the other hand, according to the solar radiation trend, higher electrical and thermal productions are obtained. The PVT thermal efficiency reaches the maximum value equal to 26%, between 10:00 and 11:00 a.m. In this time horizon, the peaks of electricity productions are also obtained, equal to 0.7 kW for the PVT and to 1.1 kW for the PV panels.

Finally, Figure 8 shows the PVT outlet and inlet fluid temperature and PV operating temperature during a summer sample day. Here, it is clearly shown that, during summer, the PVT outlet fluid temperatures reach 40 °C, whereas during winter operation (not shown for sake of brevity), they reach about 25 °C. For this reason, PVT collectors act only as a DHW water preheating and, as a consequence, the electric resistance inside the tank provides the auxiliary thermal energy necessary to reach the set point temperature for DHW. Note that PV operating temperature, T,PV, is very high, reaching almost 53 °C, whereas the operating temperature of the PV cells of the PVT collectors cannot be plotted, being not recorded within the TRNSYS type.

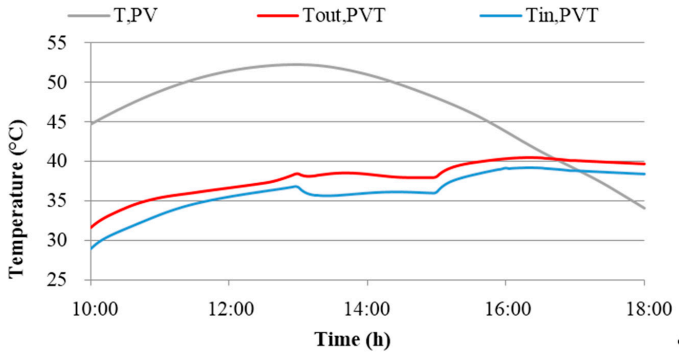

Figure 8. Summer day: inlet and outlet PVT collector temperature.

4.2. Experimental Results

4.2.1. Thermographic Analysis

By means of the infrared camera, the PV and PVT panels temperatures were measured. Figure 9 shows the PV (Figure 9a) and PVT (Figure 9b) panels temperatures measured on a typical summer day.

As it is possible to observe, the PV module reaches the maximum temperature of approximately 42 °C, whereas a lower temperature, equal to 34 °C, is reached by the PVT collector, showing the effectiveness of the fluid lowering the PVT module temperature.

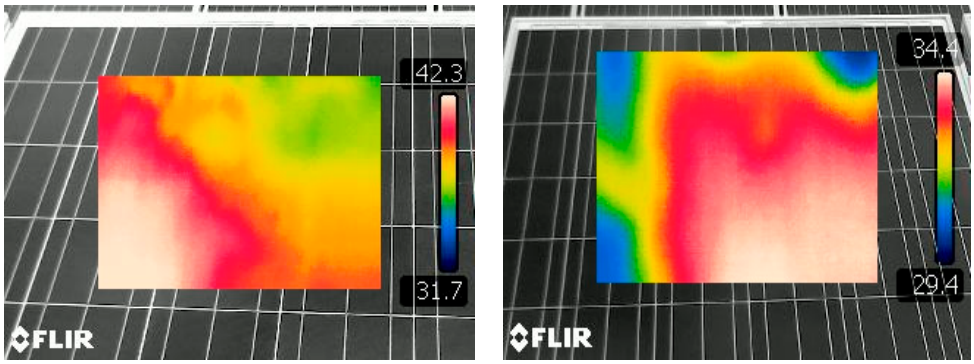

(**a**) (**b**)

Figure 9. PV panel (**a**) and PVT collector (**b**) temperature by thermal imaging camera.

Figure 10 shows the outlet water flow rate temperature of the PVT collectors entering a tee piece. The outlet water temperature, about 38 °C, is higher than the inlet one (at the bottom of the collector), highlighting the thermal exchange that occurs between the fluid and the plate, reducing the overheating of the PV cells.

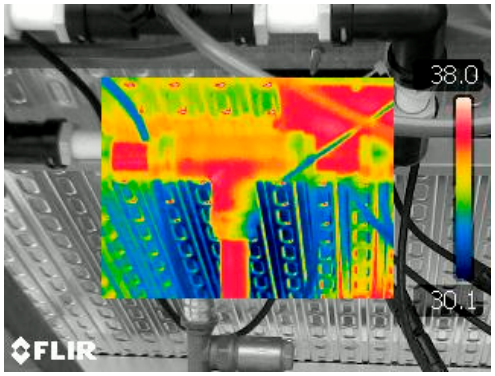

Figure 10. Detail of a tee piece of the PVT collector by thermal imaging camera.

4.2.2. Thermal Analysis

Through the experimental analysis carried out on the investigated set-up, relevant data of the system operation, such as the ambient temperature (T_{amb}), the PV panel (T PV) and PVT collector (T PVT) temperature, the PVT inlet (T_{in}, PVT) and outlet (T_{out}, PVT) water temperature and the total radiation (G), are measured and stored by the data-logger. Figure 11 shows the dynamic trend of all those parameters for the same summer sample day selected for the numerical analysis. Between 12:00 a.m. and 6:00 p.m., the PVT collector temperature is averagely around 33 °C, being lower than the PV panel one, which reaches almost 50 °C during the hottest hours of the day (11 a.m.–4:00 p.m.). It is worth noting that T PV also shows a remarkable temperature fluctuation, also due to a poor response of the panel to the solar radiation fluctuation/reduction (cloudy sky). Nevertheless, the temperature difference, T PV–T PVT, demonstrates the cooling effect provided in the PV cells by the heat transfer fluid flowing through the PVT collectors. For this reason, an increase of the PVT outlet temperature, T_{out},PVT, ranging between 35 and 40 °C, vs. the inlet one T_{in},PVT, ranging between 31 and 38 °C, is observed. The obtained average thermal efficiency of PVT collectors (not shown for the sake of brevity) is around 15%.

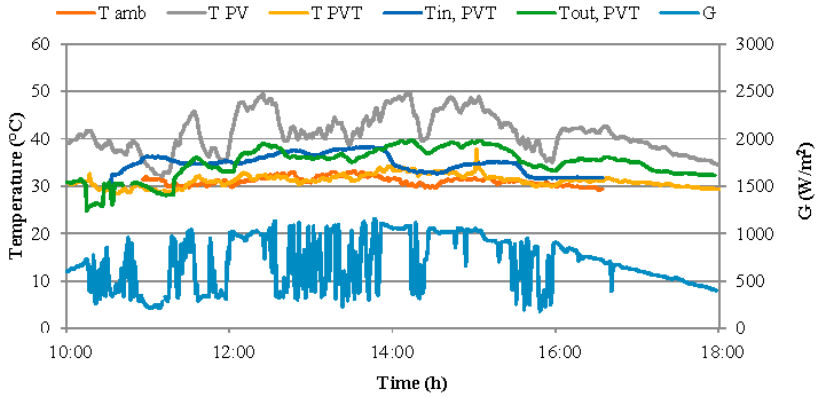

Figure 11. Ambient temperature, PVT and PV temperature, total radiation.

4.2.3. Electrical Analysis

The measured electrical data of PV panels and PVT collectors were obtained by the SolarEdge, a real-time performance monitoring system able to record the electrical parameters (power, voltage, current, energy, etc.), enabling logical and physical PV site visualization with real-time performance data for each individual module and for the whole system. All data were logged, thenreviewed and analyzed at any time from any location thanks to the remote service capabilities. Figure 12a, for a summer operation day, shows the recorded data of a PV panel and of a PVT collector are shown.

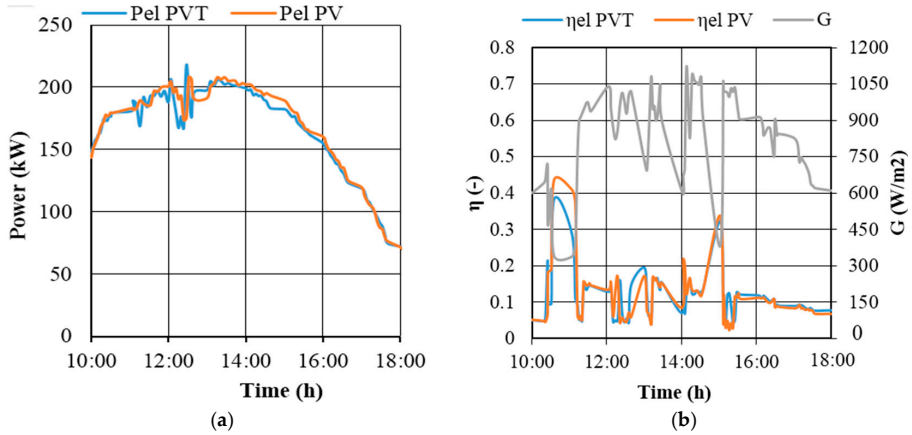

Figure 12. PVT collector and PV panel daily power (**a**) and efficiency (**b**).

Here, it is possible to note that the PV panel power (Pel PV) and PVT collector one (Pel PVT) coincide. Some fluctuations of the recorded data are due to the cloudy sky occurring during the data recording. On the right side of Figure 12 the calculated electrical efficiency of both the system are reported together with the incident solar radiation. ηel PV and ηel PVT collector range between 5% to about 45%, and small differences between them are observed. The electrical efficiency dramatically decreases when high solar radiation values overheat the PV cells, resulting in a reduction of the PV efficiency. On the other hand, despite the considerable temperature difference observed between the PV panel and the PVT collector (e.g., Figure 11), the PVT efficiency increases only in the case of optimal conditions in terms of solar radiation and collector temperature.

5. Conclusions

The presented paper focuses on the assessment of the energy and economic performance of an experimental set-up, consisting of a solar system including PV panels and PVT collectors for the

production of electricity and domestic hot water. The design and the installation of the set-up and the dynamic simulation model are analyzed, described and discussed. The set-up is installed at AV Project Ltd., located in Avellino (Italy). The plant is monitored by suitable sensors such as flowmeter, pyranometer, thermoresistances and thermocouples, power optimizer and controlled by a real time monitoring system. A simulation model of the plant was developed in TRNSYS environment with the aim to assess the energy and economic performance of the reference PVT technology (i.e., glazed collectors), also compared with the tested PV technology. The obtained numerical results show that:

- the electrical energy produced by the PV panels (1778 kWh/year) is higher than the PVT one (1156 kWh/year). Obviously, PVT collectors also produce a significant amount of thermal energy (1433 kWh/year);
- a PV electrical efficiency equal to 17.9% is obtained, whereas PVT collectors show a global efficiency of 26%, sum of the electrical efficiency of 11.6% and the thermal one of 14.4%;
- during summer operation, PVT outlet temperatures often reach 40 °C, whereas during winter, PVT collectors are mainly used to preheat the water, heated up to the DHW set point temperature by the auxiliary electric resistance;
- the economic profitability of the both investigated systems (PV and PVT systems) in the case of capital cost contribution (50% of total capital cost), is positive. A SPB of about 4 years is obtained.

Similarly, the obtained experimental results show that:

- a considerable temperature difference, about 10 °C, is observed between PV panels and PVT collectors;
- the average electrical efficiencies of PV and PVT collectors are almost coincident and range around 15%;
- the average thermal efficiency of PVT collectors is around 13%, significantly lower than the efficiency obtained by solar collector at the same operating conditions.

Author Contributions: All authors contributed equally to this work, they also revised and approved the manuscript.

Conflicts of Interest: The authors declare no conflict of interest.

Abbreviations

The following abbreviations are used in this manuscript:

A	Solar Collector Area (m^2)
AF	Annuity Factor (−)
C	Capital Cost (€)
E	Energy (kWh/year)
G	Radiation (kW), (W/m^2)
I	Current (A)
LCV	Lower Calorific Value (kWh/Sm^3)
NOCT	Nominal Operating Cell Temp. (°C)
k	Boltzmann constant (J/K)
P	Power (kW)
q	electron charge constant (−)
V	Voltage (V)
Greeks Letters	
η	Efficiency (−)
Δ	Difference (−)
Subscripts and Superscripts	
DHW	Domestic Hot Water
el	electrical
GB	Gas Boiler
HE	Heat Exchanger

in	inlet
M	Maintenance (€/year)
mp	max power
ng	naural gas
oc	short-circuit
out	outlet
PVT	PhotoVoltaic/Thermal
Ref	Reference Conditions
RS	Reference System
sc	short-circuit
SCF	the Solar Collector Fluid
th	thermal
TK	Storage Tank
tot	total
TW	Tap Water

References

1. Bougiatioti, F.; Michael, A. The architectural integration of active solar systems. Building applications in the Eastern Mediterranean region. *Renew. Sustain. Energy Rev.* **2015**, *47*, 966–982. [CrossRef]
2. Dusonchet, L.; Telaretti, E. Comparative economic analysis of support policies for solar PV in the most representative EU countries. *Renew. Sustain. Energy Rev.* **2015**, *42*, 986–998. [CrossRef]
3. Chow, T.T. A review on photovoltaic/thermal hybrid solar technology. *Appl. Energy* **2010**, *87*, 365–379. [CrossRef]
4. Zondag, H.A. Flat-plate PV-Thermal collectors and systems: A review. *Renew. Sustain. Energy Rev.* **2008**, *12*, 891–895. [CrossRef]
5. Shan, F.; Tang, F.; Cao, L.; Fang, G. Performance evaluations and applications of photovoltaic-thermal collectors and systems. *Renew. Sustain. Energy Rev.* **2014**, *33*, 467–483. [CrossRef]
6. Aste, N.; Leonforte, F.; del Pero, C. Design, modeling and performance monitoring of a photovoltaic-thermal (PVT) water collector. *Sol. Energy* **2015**, *112*, 85–99. [CrossRef]
7. Bilbao, J.I.; Sproul, A.B. Detailed PVT-water model for transient analysis using RC networks. *Sol. Energy* **2015**, *115*, 680–693. [CrossRef]
8. Kim, J.-H.; Park, S.-H.; Kang, J.-G.; Kim, J.-T. Experimental performance of heating system with building-integrated PVT (BIPVT) collector. *Energy Proced.* **2014**, *48*, 1374–1384. [CrossRef]
9. Kumar, A.; Baredar, P.; Qureshi, U. Historical and recent development of photovoltaic thermal (PVT) technologies. *Renew. Sustain. Energy Rev.* **2015**, *42*, 1428–1436. [CrossRef]
10. Skoplaki, E.; Palyvos, J.A. On the temperature dependence of photovoltaic module electrical performance: A review of efficiency/power correlations. *Sol. Energy* **2009**, *83*, 614–624. [CrossRef]
11. Sandnes, B.; Rekstad, J. A photovoltaic/thermal (PV/T) collector with a polymer absorber plate. Experimental study and analytical model. *Sol. Energy* **2002**, *72*, 63–73. [CrossRef]
12. Fraisse, G.; Ménézo, C.; Johannes, K. Energy performance of water hybrid PV/T collectors applied to combisystems of direct solar floor type. *Sol. Energy* **2007**, *81*, 1426–1438. [CrossRef]
13. Tyagi, V.V.; Kaushik, S.C.; Tyagi, S.K. Advancement in solar photovoltaic/thermal (PV/T) hybrid collector technology. *Renew. Sustain. Energy Rev.* **2012**, *16*, 1383–1398. [CrossRef]
14. Kalogirou, S.A.; Tripanagnostopoulos, Y. Hybrid PV/T solar systems for domestic hot water and electricity production. *Energy Convers. Manag.* **2006**, *47*, 3368–3382. [CrossRef]
15. Touafek, K.; Khelifa, A.; Adouane, M. Theoretical and experimental study of sheet and tubes hybrid PVT collector. *Energy Convers. Manag.* **2014**, *80*, 71–77. [CrossRef]
16. Fan, J.; Seng, T.P.; On, L.K.; Hua, G.L. Experimental study on glazed mc-Si solar photovoltaic/thermal(PVT) system. *Energy Proced.* **2014**, *61*, 2787–2790. [CrossRef]
17. Herrando, M.; Markides, C.N. Hybrid PV and solar-thermal systems for domestic heat and power provision in the UK: Techno-economic considerations. *Appl. Energy* **2016**, *161*, 512–532. [CrossRef]
18. Herrando, M.; Markides, C.N.; Hellgardt, K. A UK-based assessment of hybrid PV and solar-thermal systems for domestic heating and power: System performance. *Appl. Energy* **2014**, *122*, 288–309. [CrossRef]
19. Guo, C.; Ji, J.; Sun, W.; Ma, J.; He, W.; Wang, Y. Numerical simulation and experimental validation of tri-functional photovoltaic/thermal solar collector. *Energy* **2015**, *87*, 470–480. [CrossRef]

20. Sardarabadi, M.; Passandideh-Fard, M.; Zeinali Heris, S. Experimental investigation of the effects of silica/water nanofluid on PV/T (photovoltaic thermal units). *Energy* **2014**, *66*, 264–272. [CrossRef]
21. Klein, S.A.; Beckman, W.A.; Mitchell, J.W.; Duffie, J.A.; Duffie, N.A.; Freeman, T.L.; MItchell, J.C.; Braun, J.E.; Evans, B.L.; Kummer, J.P.; et al. *TRNSYS. A Transient System Simulation Program*; University of Wisconsin: Madison, WI, USA, 2006.
22. Buonomano, A.; Calise, F.; Ferruzzi, G.; Vanoli, L. A novel renewable polygeneration system for hospital buildings: Design, simulation and thermo-economic optimization. *Appl. Therm. Eng.* **2014**, *67*, 43–60. [CrossRef]
23. Buonomano, A.; Calise, F.; Ferruzzi, G. Thermoeconomic analysis of storage systems for solar heating andcooling systems: A comparison between variable-volume andfixed-volume tanks. *Energy* **2013**, *59*, 600–616. [CrossRef]
24. Duffie, J.A.; Beckman, W.A. *Solar Engineering of Thermal Processes*; John Wiley & Sons, Inc.: New York, NY, USA, 1991.
25. Eckstein, J.H. Detailed Modeling of Photovoltaic Components. Master's Thesis, Solar Energy Laboratory, University of Wisconsin, Madison, WI, USA, 1990.
26. Townsend, T.U. A Method for Estimating the Long-Term Performance of Direct-Coupled Photovoltaic Systems. Master's Thesis, Solar Energy Laboratory, University of Wisconsin, Madison, WI, USA, 1989.
27. Florschuetz, L.W. Extension of the Hottel-Whillier-Bliss model to the analysis of combined photovoltaic/thermal flat plate collectors. *Sol. Energy* **1976**, *6*, 79–92.
28. Evans, D.L.; Facinelli, W.A.; Otterbein, R.T. *Combined Photovoltaic/Thermal System Studies*; Report ERC-R-78017; Arizona State University: Tempe, AZ, USA, 1978.
29. Allan, J.; Dehouche, Z.; Stankovic, S.; Mauricette, L. Performance testing of thermal and photovoltaic thermal solar collectors. *Energy Sci. Eng.* **2015**, *3*, 310–326. [CrossRef]

© 2016 by the authors; licensee MDPI, Basel, Switzerland. This article is an open access article distributed under the terms and conditions of the Creative Commons Attribution (CC-BY) license (http://creativecommons.org/licenses/by/4.0/).